Dynamic analysis of partially saturated river embankment considering liquefaction using a multiphase coupled FEM analysis method

Sayuri Kimoto[1], H. Yui[2], and F. Oka[3]

[1] Department of Civil and Earth Resources Engineering, Kyoto University, Kyoto, 615-8540, Japan.
[2] Nikken Sekkei Civil Engineering Ltd., Former MS student of Kyoto University, Osaka, 541-0054, Japan.
[3] Professor Emeritus of Kyoto University, Association for Disaster Prevention Research, Kyoto, 606-8226, Japan

ABSTRACT

In this paper, dynamic analyses considering liquefaction were conducted for the partially saturated river embankment using a multiphase coupled FEM analysis method. An elastoplastic model considering the effect of suction and an elasto-viscoplastic model were used for the constitutive equations for partially saturated sand and clayey soils, respectively. The seismic behavior of embankments on a clayey subsoil layer was investigated through the simulations by the proposed method. In particular, the authors focused on the deformation behavior of partially saturated river embankment due to the liquefaction of the soils inside the embankment and the effect of the thickness of saturated sand layer on the crown settlement. It is found that there is a linear relation between the crown settlement and the thickness of the saturated sand layer.

Keywords: partially saturated soil; embankment; liquefaction; dynamic analysis

1 INTRODUCTION

It is known that the severe damages of river dikes, such as, large settlement of crown and lateral spreading, are accompanied by soil liquefaction in most cases. The cause of the damage of embankments induced by soil liquefaction can be roughly classified into two types, i.e., a liquefaction of the foundation ground and that of the soil inside the embankment. It has been reported that damage of river embankments in Tohoku districts due to the 2011 off the Pacific Coast of Tohoku Earthquake was typically classified into the latter case. This type of failure mechanism is explained by the existence of saturated loose soil layer in the embankment due to relatively high groundwater level inside the embankment, and the settlement of constructed embankments into the foundation by the self-weight induced consolidation.

In the present study, dynamic behaviors of river embankments with liquefiable layer inside the embankment have been simulated and discussed using a three-phase coupled FEM analysis method based on the finite deformation theory.

2 GOVERNING EQUATIONS

The governing equations of dynamic analysis for multiphase geomaterials, i.e., air-water-soil three phase materials, are described within the framework of theory of porous media. In the theory, the governing equations are described for the multiphase mixture, i.e., an immiscible mixture of solid and fluids (Oka and Kimoto, 2012). The u-p formulation based on the updated Lagrangian method has been employed along with the Jaumann rate of Cauchy stress tensor for the weak form of the equilibrium equation to deal with large deformation. An elastoplastic constitutive model and an elasto-viscoplastic constitutive model considering nonlinear kinematic hardening were used to describe plastic and viscoplastic behaviors of soil skeleton during cyclic loading, respectively. In addition, a soil-water characteristic curve was used as a constitutive equation.

The formulations of the finite deformation analysis by Oka et al. (2018) and the three-phase porous theory for the unsaturated soil by Kato et al. (2014) were combined to derive the governing equations in the present study. The detailed descriptions for the dynamic finite element formulations are shown in Shahbodagh Khan (2011) and Oka et al. (2018).

2.1 Partial stresses for the mixture

The total stress tensor is assumed to be composed of three partial stress values as:

$$\sigma_{ij} = \sigma_{ij}^{S} + \sigma_{ij}^{W} + \sigma_{ij}^{G} \tag{1}$$

where σ_{ij} is the total stress tensor, and σ_{ij}^{S}, σ_{ij}^{W}, and σ_{ij}^{G} are the partial stress tensors for solid, water, and air, respectively. Considering the volume fraction, the partial stress tensors for partially saturated soils can be given by

$$\sigma_{ij}^{S} = \sigma'_{ij} - n^{S} P^{F} \tag{2}$$

$$\sigma_{ij}^{W} = -n^{W} P^{W} \delta_{ij} \tag{3}$$

$$\sigma_{ij}^{G} = -n^{G} P^{G} \delta_{ij} \tag{4}$$

$$P^{F} = S_r P^{W} + (1 - S_r) P^{G} \tag{5}$$

where P^W and P^G are the pore water pressure and the pore air pressure, respectively, P^F is the average pore pressure, $S_r = n^W / (n^W + n^G)$ is the degree of water saturation, and δ_{ij} is the Kronecker's delta. σ'_{ij} is the skeleton stress tensor, and the tension is positive for stresses in the formulation. n^S, n^W, and n^G are the volume fractions of soil, water, and gas phases, respectively. Substituting Eqs. (2) – (5) into Eq. (1) yields

$$\sigma'_{ij} = \sigma_{ij} - P^{F} \delta_{ij} \tag{6}$$

In the present study, the skeleton stress tensor is used as the basic stress variable in the constitutive model of the soil skeleton, and the suction is used in the constitutive model which describes a bonding effect.

2.2 Constitutive equations

An elastoplastic constitutive model by Oka et al. (1999) and an elasto-viscoplastic constitutive model by Kimoto et al. (2015) are used for the saturated sandy soil and the saturated clayey soil, respectively. An extended elastoplastic model considering the effect of suction (Kato et al. 2014) is used for the partially saturated sand.

The soil-water characteristic curve for soil describes the relationship between the volumetric water content or the degree of saturation and the suction of the soil. The curve can be obtained as a measure of the water-holding capacity of the soil as the water content changes when it is subjected to various levels of suction. In the model, the equation proposed by van Genuchten (1980) is adopted.

2.3 Conservation laws and discretization

The mass conservation laws for the three phases, that is, solid, water, and gas phase, are considered. In addition, the conservation laws of the linear momentum for the three phases are used. The sum of the conservation laws of linear momentum for the three phases gives the equation of motion for the whole multiphase mixture.

The weak form of the continuity equation for water and gas, the equation of motion are discretized in space by the finite element method. Assuming two dimensional plane strain condition, an 8-node isoparametric element is used for the displacement, velocity and acceleration of the solid skeleton, and 4-node isoparametric element is used for pore water pressure and pore gas pressure. For the time discretization, Newmark's method is adopted. In the following calculations, $\beta = 0.3025$, $\gamma = 0.6$, and the calculation time increment $\Delta t = 0.001$ sec were used. It should be mentioned that the pore-air pressure is assumed to be zero in the following simulations since the effect of pore-air pressure was found to be negligible under drained conditions at the surface boundary.

3 DYNAMIC ANALYSIS OF EMBANKEMENT

3.1 Simulation model

Fig. 1 shows the finite element meshes with boundary conditions for the simulations. The typical river embankment on the clay foundation was modeled. The height of the embankment from the ground surface is 6.0 m, and the inclination of the slope is set to be 1:2. To reduce the side boundary effects, semi-infinite elements with equi-displacement conditions were used on the left and right ends. The rigid base is used so that the bottom boundary of the model is fixed. Simulation cases are shown in Table 1 and the geometry of the embankment model is depicted in Fig. 2. Total seven cases with different ground profiles were simulated. Cases 2-1, 2-2, 2-3, 2-4 correspond to the case in which the bottom of the embankment has settled into the clayey subsoil layer, and the water table exists inside the embankment body in upward convex shape. The maximum thickness of the saturated zone inside the embankment is from 1.0 m to 3.3 m. Case 2-5 corresponds to the case in which the embankment has not settled and the water table exists inside the embankment body in upward convex shape.

The embankment body over the saturated zone is assumed to be made of the partially saturated sandy soil with maximum saturation of 60%. The initial pore water pressure below the water table is given by the hydrostatic pressure. The pore water pressure and the pore air pressure on the boundaries of the embankment is assumed to be zero. Fig. 3 shows an input earthquake motion record used in this analysis. The acceleration profile was obtained during the 2011 off the Pacific Coast of Tohoku Earthquake and it was recorded at a depth of 80 m at Tajiri in Miyagi Prefecture (MYGH06, KiK-net) with a maximum acceleration of 152.2 gal.

The elastoplastic model and the elasto-viscoplastic model are used for the embankment soil and the clayey foundation, respectively. The material parameters of the sandy soil were determined based on the experimental data of the loose sand at the Akita port damaged due to liquefaction, and the parameters of the soft clay were determined based on the data for alluvial clay at Torishima along Yodo River. The cyclic strength curves for each soil are shown in Fig. 4, and the soil-water characteristic curve by the van Genuchten type model for sand layer is shown in Fig. 5.

Table 1. Simulation cases.

Case	Water table	Top of water table	Settlement depth	Thickness of saturated sand
1-1	flat	GL -1.5m	-	-
1-2	flat	GL -1.5m	1.0 m	1.0 m

2-1	parabola	GL +0.0m	1.0 m	2.5 m
2-2	parabola	GL +0.8m	1.0 m	3.3 m
2-3	parabola	GL +0.0m	0.5 m	2.0 m
2-4	parabola	GL +0.5m	0.5 m	2.5 m
2-5	parabola	GL +1.0m	-	2.5 m

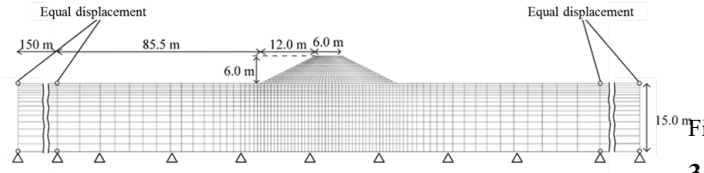

Fig. 1. Finite element meshes.

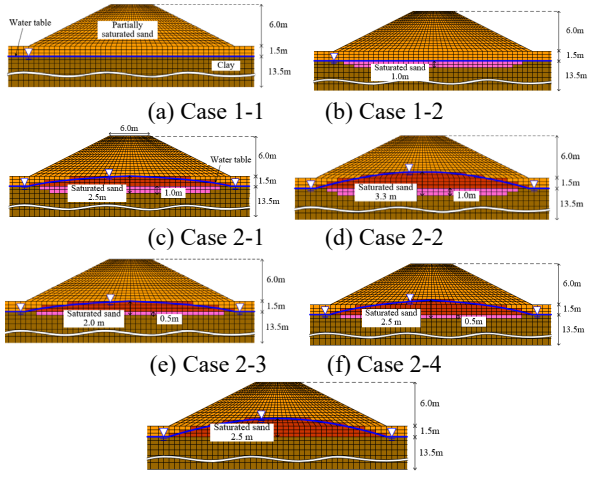

Fig. 2. Soil profiles for each case.

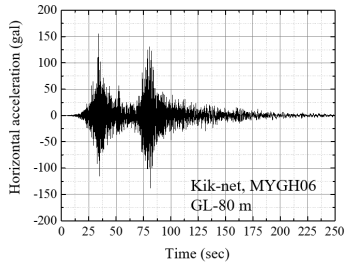

Fig. 3. Input acceleration (MYGH06, KiK-net).

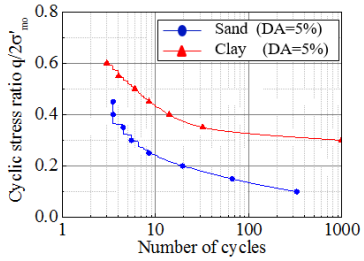

Fig. 4. Cyclic strength curves of materials.

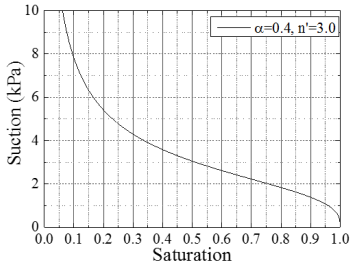

Fig. 5. Soil-water characteristic curve for sand.

3.2 Simulation results

First, the results of Case 2-2 in which the thickness of the saturated sand is 3.3 m are shown to discuss the typical behavior of embankment with liquefaction of the soils inside the levee. The distributions of the skeleton stress decreasing ratio (SSDR) which is defined by $(\sigma'_{m0}-\sigma'_{m})/\sigma'_{m0}$ and gives the degree of liquefaction are shown in Fig. 6. Liquefaction of the water-saturated region in the embankment can be seen at 66s after the earthquake. Fig. 7 shows the distribution of the degree of saturation. The degree of saturation increases inside the embankment in the region where the suction decreases. The accumulated plastic deviatoric strain are presented in Fig. 8. The localization of the accumulated plastic shear strain from the top of the slope, that is, slip failure, can be seen at 66s after the earthquake. In addition, the large strain is obtained in the liquefied region beneath the water table. At 200s after the earthquake, the shear localization can be seen in several regions and the complex deformation occurs in the embankment.

The vertical and horizontal displacement-time profile at the top are compared for Cases 2-1, 2-2, 2-3 in Fig. 10. The larger settlement was obtained for the case with larger thickness of the saturated sand layer. The vertical and horizontal displacement-time profile at the toe of the embankment are shown in Fig. 11. The largest lateral spreading is seen for Case 2-2. The settlement rate, that is, the ratio of settlement to the height of the embankment, is summarized for all the calculation cases in Fig. 12. The linear relations can be seen between the thickness of the saturated sand and the settlement rate irrespective of the position of water table.

4 CONCLUSION

Dynamic analyses of partially saturated river embankment using a multiphase coupled FEM analysis method were presented. The localization of the shear strain was observed in several regions and the complex deformation occurred in the embankment due to the liquefaction of sandy soil in the embankment. By comparing the results of the cases with different thickness of saturated sandy layer, the linear relation was obtained between the thickness of the saturated sand layer and the settlement rate.

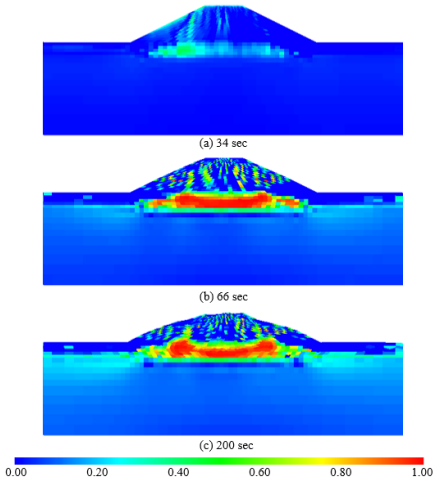

Fig. 6. Distribution of skeleton stress decreasing ratio (Case 2-2).

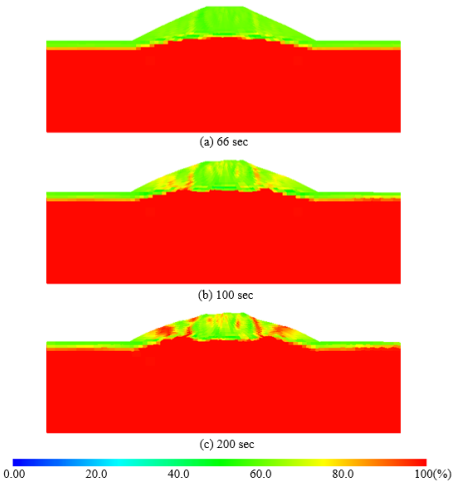

Fig. 7. Distribution of saturation (Case 2-2).

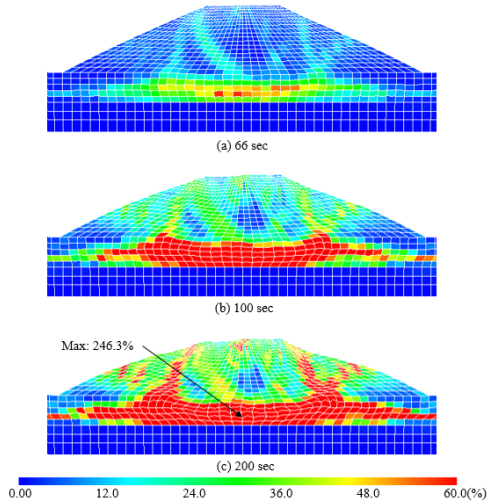

Fig. 8. Distribution of accumulated plastic/viscoplastic deviatoric strain (Case 2-2).

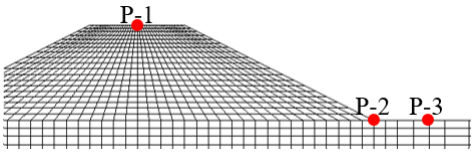

Fig. 9. Position of output for the displacement.

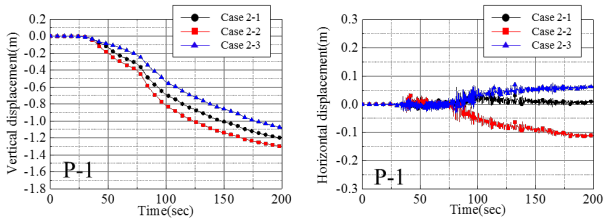

Fig. 10. Vertical and horizontal displacement-time profile at the top (Case 2-1, 2-2, 2-3).

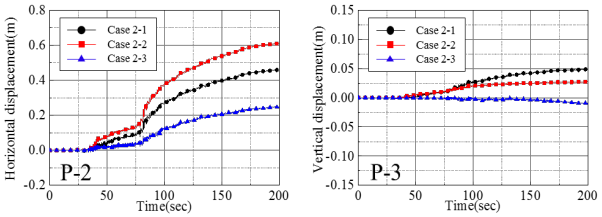

Fig. 11. Vertical and horizontal displacement-time profile at the toe (Case 2-1, 2-2, 2-3).

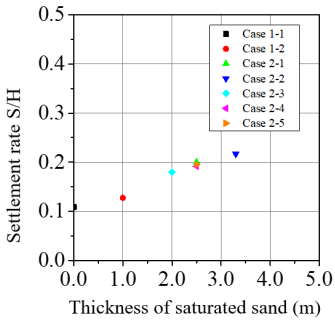

Fig. 12. Relations between the thickness of the saturated sand layer and the settlement rate.

REFERENCES

Kato, R., Oka, F. and Kimoto, S. (2014). A numerical simulation of seismic behavior of highway embankments considering seepage flow, Computer methods and Recent Advances in Geomechanics, Proc. of the 14th Int. Conf. of International Association for Computer Methods and Recent Advances in Geomechanics, Kyoto, Japan, 22-25 September, 755-760.

Kimoto, S., Sahbodagh, K.B., Mirjalili, M., Oka, F. (2015). A cyclic elastoviscoplastic constitutive model for clay considering the nonlinear kinematic hardening rules and the structural degradation, Int. J. Geomechanics, 15(5), A4014005.

Oka, F., Yashima, A., Tateishi, A., Taguchi, Y., Yamashita, S. (1999). A cyclic elasto-plastic constitutive model for sand considering a plastic-strain dependence of the shear modulus, Geotechnique, 49 (5), 661-680.

Oka, F. and Kimoto, S. (2012). Computational modeling of multi-phase gematerials, CRC press, Taylor & Francis group.

Oka, F, Shahbodagh Khan, B. and Kimoto, S. (2018). A computational model for dynamic strain localization in unsaturated elasto-viscoplastic soils, Int. J. Numer. Anal. Methods Geomech., (accepted in August, 2018).

Shahbodagh Khan, B. (2011). Large deformation dynamic analysis method for partially saturated elasto-viscoplastic soils, Ph.D. thesis, Kyoto University.

Van Genuchten MT. (1980). A closed-form equation for predicting the hydraulic conductivity of unsaturated soils. Soil Science Society of American Journal, 44, 892–898.